*Concepts and Modelling in Geomorphology: International Perspectives*,
Eds. I. S. Evans, R. Dikau, E. Tokunaga, H. Ohmori and M. Hirano, pp. 185–197.


# A Simple GIS Model for Mapping Landslide Susceptibility

Richard J. PIKE, Russell W. GRAYMER and Steven SOBIESZCZYK

*U.S. Geological Survey, 345 Middlefield Road, Menlo Park, CA 94025, U.S.A.*
*e-mail: rpike@usgs.gov*

**Abstract.** Digital maps of geology, ground slope, and dormant landslides are combined statistically in a geographic information system (GIS) to identify sites of future landsliding over a broad area. The resulting index number, a continuous variable, predicts a range of susceptibility both within and between existing landslides. Spatial resolution of the index can be as fine as that of the slope map, and areal coverage is limited only by the extent of the input data. Susceptibility is defined for each geologic-map unit as the *spatial frequency* of the unit occupied by dormant landslides, adjusted locally by ground slope. Susceptibility of terrain between landslides is calculated for each one-degree slope interval as the percentage of grid cells that coincide with the failures. Susceptibility within landslides is the same percentage times the comparative frequency of recent failures within and outside the old landslides. We tested the model in an 872 $km^2$ urban area in California, using 120 geologic units, a 30-m digital elevation model, 6714 dormant landslide deposits, 1192 recent landslides, and ARC/INFO software. The method could generate a similar map for any area where the necessary digital-map data are available.

**Keywords:** Geomorphic Hazards, Landslide Susceptibility, Statistical Mapping, GIS, DEM

## INTRODUCTION

Landslides pose a hazard to life and property worldwide. Improving public safety by predicting unstable slopes—in time or space, locally or regionally—is a complex problem in applied geomorphology for which many solutions have been proposed. One of the best clues to the location of future landsliding is the mapped distribution of past failures (Radbruch and Crowther, 1970; Nilsen and Wright, 1979). Such an *inventory* of landslides reveals the extent of prior movement and the probable locus of some future activity in the area, but it is discontinuous. An inventory does not indicate the likelihood of failure for the much broader expanses of terrain between landslides. By numerically (if manually) combining maps of geology, an inventory of Quaternary landslides, and generalized estimates of slope gradient, Brabb *et al*. (1972) first modeled the widely varying predisposition, or *susceptibility*, of hillside terrain to landsliding—both continuously and over a large area.

The semi-quantitative approach of Brabb *et al*. (1972) is extended here. Advances include higher-resolution data on geology and slope gradient, a fully numerical method implemented in a geographic information system (GIS), and a

uniformly high spatial resolution for the resulting hazard map. In the absence of guidelines for mapping landslide susceptibility, the model is predicated on six assumptions:

- The record of past landsliding can infer the location of future instability.
- Failures under climatic conditions that no longer prevail suggest the locus of future landsliding if not necessarily its abundance or temporal frequency.
- The areal percentage of past failure in a geologic unit reflects the combination of landslide-inducing conditions and processes unique to that unit.
- Geology, slope gradient, and areas of prior failure collectively serve as a proxy for materials-properties data needed to quantify susceptibility.
- Susceptibility of dormant landslides to later movement exceeds that of the terrain between them.
- A simple analysis of the spatial frequency of recent landslides can quantify the added likelihood of renewed activity in older landslides.

The model accommodates either specific types of slope movement or, as in this chapter, a mixture of types. Because the dormant landslides in our test area were identified by airphoto interpretation rather than by field mapping, the failures could not be attributed by type of movement. More recent inventories (e.g. Wilson *et al*., 2002) do not cover the area. Lacking detailed information, we term all dormant failures "non-debris flow landslides." "Landslide" or "slide" in this study connotes a topographically recognizable deposit (excluding its source area) probably formed in bedrock by one of the deeper mechanisms (Varnes, 1978). Few of these landslides are likely to be shallow debris flows, which leave a thin, ephemeral deposit (Dietrich *et al.*, 1993).

Figure 1D, a representative result of our regional-statistical analysis, shows 9 $km^2$ of a susceptibility map of the 872-$km^2$ test site, metropolitan Oakland in the San Francisco Bay region of northern California. To prepare the larger map, Pike *et al*. (2001) divided the Oakland area into 969,003 rectangular cells 30 m on a side, the spacing of the input digital elevation model (DEM), and created four digital raster-grid maps at this resolution: geology, presence-or-absence of old landslide deposits, slope gradient, and point locations of post-1967 landslides. Susceptibility was calculated at a 30-m resolution in the GRID module of version 7.1.1 of ARC/INFO, a commercial GIS, on a SUN/Solaris UNIX computer, from a two-step algorithm written in Arc Macro Language. We have since applied the model to a larger area in the San Francisco Bay region (Pike and Sobieszczyk, 2002).

## INPUT TO THE MODEL

### *1. Geology*

Hillside materials are the dominant site control over the larger, deeper types of slope movement worldwide (Aniya, 1985; Brunori *et al*., 1996; Jennings and Siddle, 1998; Irigaray *et al*., 1999). In the Oakland test area, prevalence of landsliding varies widely among the 120 lithologic units (Graymer, 2000). These

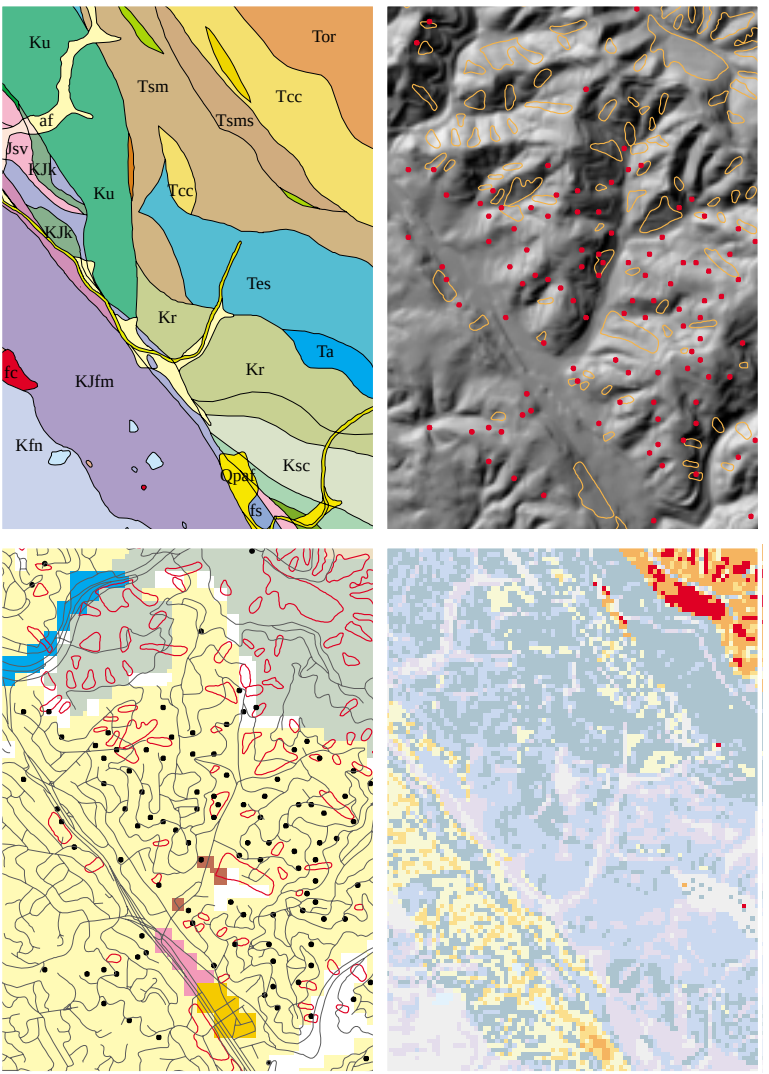


Fig. 1. Preparing a landslide-susceptibility map (after Pike *et al*., 2001). Maps for part of the city of Oakland, California, are about 2 km across. A, upper left. Geology; 19 units in Table 1. NNW-striking Hayward Fault Zone is at eastern edge of unit KJfm. B, upper right. Inventory of old landslide deposits (orange polygons) and locations of post-1967 landslides (red dots) on uplands east of the fault and on gentler terrain to the west. Shaded relief from 10-m DEM. C, lower left. Landslides and old deposits on 1995 land use (100-m resolution). Yellow, residential; green, forest; tan, scrub; blue, major highway; pink, school; orange, commercial; brown, public institution; white, vacant and mixed use; road net in gray. D, lower right. Values of relative susceptibility at 30-m resolution mapped in eight intervals from low to high as gray, 0.00; purple, 0.01–0.04; blue, 0.05–0.09; green, 0.10–0.19; yellow, 0.20–0.29; light-orange, 0.30–0.39; orange, 0.40–0.54; red, ≥0.55. Values 0.05–0.20 predominate in this small 9 $km^2$ sample of the Oakland study area.

Table 1. Data on dormant landslide deposits and post-1967 landslides for 20 selected geologic units in the Oakland metropolitan area, California—arrayed by mean spatial frequency. Spatial frequencies by slope gradient are shown for two units in Fig. 2.

| GEOLOGIC UNIT | | | OLD LANDSLIDE DEPOSITS | | POST-1967 LANDSLIDES | |
|---|---|---|---|---|---|---|
| Map symbol | Name (after Graymer, 2000) | All cells (number of 30-meter grid cells) | Landslide cells (number of grid cells) | Mean spatial frequency (Landslide cells / All cells) | Total number (one grid cell per landslide) | Number on old landslide deposits |
| Kfa | † Franciscan Complex - Alcatraz terrane | 1002 | 820 | ***0.82*** | 6 | 6 |
| Tor | Orinda Formation (Miocene) | 35166 | 9682 | ***0.28*** | 83 | 27 |
| KJfm | Franciscan Complex mélange - undivided | 12212 | 2559 | ***0.21*** | 66 | 19 |
| Tsm | unnamed glauconitic mudstone | 3389 | 438 | ***0.13*** | 24 | 0 |
| Tsms | x unnamed glauconitic mudstone - siltstone and ss | 362 | 46 | ***0.13*** | 3 | 0 |
| Tcc | Claremont Chert | 10590 | 1177 | ***0.11*** | 4 | 0 |
| Ksc | Shephard Creek Formation | 5675 | 508 | ***0.09*** | 12 | 1 |
| KJk | Knoxville Formation | 8164 | 663 | ***0.08*** | 25 | 1 |
| Jsv | keratophyre, qtz. keratophyre above ophiolite | 15627 | 1212 | ***0.08*** | 50 | 6 |
| Ku | Great Valley sequence - undifferentiated | 12706 | 965 | ***0.08*** | 35 | 2 |
| Kr | Redwood Canyon Formation (Cretaceous) | 27503 | 1697 | ***0.06*** | 27 | 1 |
| Tes | Escobar Sandstone (Eocene) | 2513 | 141 | ***0.06*** | 43 | 3 |
| fs | Franciscan Complex sandstone | 3441 | 109 | ***0.03*** | 9 | 1 |
| Ta | x unnamed glauconitic sandstone | 163 | 3 | ***0.02*** | 4 | 0 |
| Qpaf | Q alluvial fan and fluvial deposits (Pleistocene) | 61867 | 1010 | ***0.02*** | 87 | 0 |
| Kfn | Franciscan Complex - Novato Quarry terrane | 7879 | 122 | ***0.02*** | 27 | 1 |
| Ko | Oakland Conglomerate (Cretaceous) | 20921 | 301 | ***0.01*** | 6 | 0 |
| fc | x Franciscan Complex chert | 323 | 1 | ***0.00*** | 0 | 0 |
| Qhaf | Q alluvial fan and fluvial deposits (Holocene) | 125014 | 254 | ***0.00*** | 38 | 0 |
| af | Q artificial fill (Historic) | 65934 | 15 | ***0.00*** | 5 | 0 |
| | **‡ Totals are for all 120 geologic units** | **969,003** | **116,360** | ***0.12*** | **1192** | **183** |

† Unit Kfa, the most highly susceptible unit in the Oakland study area, does not crop out in Figure 1A

x 3 of 32 hillside units with < 450 cells, for which distributions of spatial frequency are less regular than those of other units

Q 3 of the 20 Quaternary units in flatland terrain; most are less susceptible than the 20 (of 100 total) hillside units listed here

‡ Totals on last line are for entire Oakland study area, not just the small sample area in Figure 1 (Pike et al., 2001, Table 1)

differences are evident in the contrasting values of *mean spatial frequency*, the areal percentage of landslides in a geologic unit (see sample of 20 units in Table 1; the 19 in Fig. 1A plus unit Kfa). Failed hillsides are abundant (28%), for example, in the Miocene Orinda Formation (Tor) and similarly clay-rich rocks, but much less so (11%) in the Miocene Claremont Chert (Tcc)—which differs in composition, texture, and other properties (Nilsen *et al.*, 1976; Keefer and Johnson, 1983; Graymer, 2000).

The geologic input to our susceptibility model is a digital-map database compiled for the structurally complex Oakland area by Graymer (2000) at 1:24,000 scale (Fig. 1A). The uplands in and east of the city of Oakland comprise 100 bedrock units (16 shown in Fig. 1A) that occupy 62% of the study area, range in age from Jurassic to upper Tertiary, and cover between 0.01 $km^2$ and 90 $km^2$. Dormant landslides occur in all but eight of the 100 rock units. In contrast, of the 20 unconsolidated Quaternary deposits (3 in Fig. 1A) that occupy 38% of the area, largely in flatland terrain, only five units, among them alluvial fan and fluvial deposits Qpaf and Qhaf, contain old landslides (Table 1).

*2. Old landslide deposits*

Reconnaissance mapping of 6714 dormant landslides at 1:24,000 scale by Nilsen (1973, 1975) provides ample evidence of prior instability in Oakland hillsides. Figures 1B and 1C show part of the inventory identified by stereo-interpretation of 1:20,000-scale airphotos. Only landslide deposits were mapped; scarps and other source-area features upslope of the deposited masses were excluded. The inventoried slides were not visited in the field. Because failure mechanisms are difficult to interpret reliably from airphotos alone (Wills and McCrink, 2002), the landslide deposits were unattributed by type of movement (Varnes, 1978) and causal agent—earthquake or sustained rainfall. In the Oakland area, landslides large enough to be recognized on the photos Nilsen studied tend to be rock and debris slides, rock slumps, and large earth flows. Most shallow debris flows are too small or poorly preserved to have been mapped. In appearance, the 6714 deposits range from clearly discernible and uneroded features to indistinct and degraded forms recognizable only by their characteristic shapes (Nilsen, 1973). In size, deposits vary from about 1100 $m^2$ to 4 $km^2$ although most are <100 m in the longest dimension. Many medium-size and all large deposits coalesced from smaller slide masses and tend to be morphologically more complex with increasing size. Times of initial movement range from 35 years ago to possibly 200,000 years ago.

We compiled the landslide deposits as a digital database. The original linework inked on 1:24,000-scale plastic sheets by Nilsen (1975) was scanned, converted from raster to vector form, imported into ARC/INFO, hand edited, and combined in one file. The 6714 deposits occupy 12% of the Oakland study area (Table 1), mostly in the hills northeast of the Hayward Fault Zone. The deposits cover 19% of this hilly area, defined as the 100 bedrock units, and cluster in elongate patterns (not evident in the small sample in Fig. 1B) aligned with the

regional NW-SE trend (Fig. 1A).

Heavy rainfall (Nilsen *et al.*, 1976) and earthquake (Keefer *et al.*, 1998) frequently destabilize portions of landslide deposits in the San Francisco Bay area. Most dormant slides are unlikely to again move in their entirety, but smaller deposits and parts of large masses, e.g. the Mission Peak landslide (Coe *et al.*, 1999), often remobilize. Old landslide deposits thus are judged more susceptible to future movement than comparably sloping areas outside them (Nilsen and Wright, 1979; Wieczorek, 1984). This added potential for hazard can be incorporated into susceptibility estimates, based on the proclivity of recent movements for older slides.

### *3. Recent landslides*

The only data from which to modify within-slide susceptibility in our test area are 1192 rainfall-induced failures that damaged the built environment (Nilsen *et al.*, 1976; Coe *et al.*, 1999). Because outlines of most of these post-1967 failures were not recorded, we compiled their locations as point data on 30-meter cells (Figs. 1B and 1C). The 1192 landslides are not an ideal sample because they are largely failures of cut-and-fill grading in urbanized areas, many of them in such otherwise "safe" materials as alluvial fan (Qpaf) and the Novato Quarry terrane (Kfn). These landslides thus overrepresent developed parts of the study area, especially land-use category 1 in Fig. 1C. An unbiased sample, which would include the many non-damaging (and unmapped) recent failures in the undeveloped uplands east of Oakland, is not available.

Despite this bias, distribution of the recent slides among the 120 geologic units largely mimics the prevalence of dormant landslide deposits (Pike *et al.*, 2001). The Orinda Formation (Tor) and Franciscan Complex mélange (KJfm) in Table 1 are two of the five bedrock formations that together host 40% of the 1192 recent landslides; all five have mean spatial frequencies of old slide deposits that exceed 20%. Similarly, the three Quaternary units that record the highest numbers of recent failures, including alluvial fan units Qpaf and Qhaf, are the same three surficial units with the most area in old landslide deposits. Recent failures are rare in geologic units that contain the fewest old landslide deposits; none of the Oakland area's 28 units with <6 grid cells on old landslide masses hosted any post-1967 failures (Pike *et al.*, 2001, Table 1).

### *4. Topography and slope gradient*

Topography both influences and reflects slope instability. The extent of much past landsliding can be identified by a visual appraisal of ground-surface form at scales as coarse as 1:30,000 (Nilsen, 1973), but few of the geomorphic features that are diagnostic of a landslide or tract of landslide-prone terrain translate readily into numerical criteria from which an index of susceptibility might be computed. Among these few measures is slope gradient, arguably the best topographic predictor of landslide likelihood, although the relation of landsliding to slope is complex and differs according to failure process (Lanyon

and Hall, 1983; Dietrich *et al*., 1993).

To evaluate the role of topography in non-debris flow landsliding in the Oakland area, we assigned a value of slope gradient to each GIS grid cell. Graham and Pike (1998) computed these values, in one-degree increments from a 30-m DEM, as the maximum rate of change in height for a 30-m cell within a $3 \times 3$ cell subgrid. Failed and unfailed terrain in the study area differ dramatically (Pike *et al*., 2001). Unfailed slopes are strongly skewed toward low values (the mode is at zero), whereas slopes on old landslide deposits are near-normally distributed and peak at about 16°. This value might be somewhat higher if it were possible to identify potential source areas that have yet to fail. The distribution of slope gradient for the 1192 cells hosting post-1967 landslides has the same near-Gaussian shape, although the mode (about 12°) is slightly lower (Pike *et al*., 2001). The topography in Fig. 1B is from a 10-m DEM, which results in a smoother shaded-relief image than the 30-m data (but adds no useful information to the susceptibility calculations).

## ESTIMATING SUSCEPTIBILITY

Radbruch and Crowther (1970) and Brabb *et al*. (1972) equated susceptibility of an area to landsliding with the amount of the area containing dormant failures. This quantity was computed for each of Oakland's 120 geologic units as the mean spatial frequency, the number of 30-m cells in landslide deposits divided by all cells in the unit (Pike *et al*., 2001). Resulting percentages range from 82% in the Alcatraz terrane (Kfa, part of the Franciscan Complex), to <1% in alluvial deposits Qhaf (and 25 other units in table 1 of Pike *et al*., 2001). The more susceptible of the 20 lithologies sampled here (Table 1) are bedrock units on steep upland slopes. Landslide deposits are rare in the Quaternary flatland units, among which the widespread alluvial-fan deposit Qpaf (spatial frequency only 2%) contains the most landslide cells (87, see Table 1).

### *1. Refined spatial frequencies*

The mean spatial frequency of landsliding in a geologic unit (Table 1) is much less effective a predictor of future instability than an array of frequencies calculated for different values of ground slope (Brabb *et al*., 1972). Radbruch and Crowther (1970) compiled observations showing that prevalence (variously defined) of landsliding in California increases with slope gradient, but only up to a maximum—commonly 15° to 35°—depending on mode of failure and the underlying lithology. (Rock falls, topples, and some shallow landslides occur on steeper slopes; debris-flow source areas, for example, peak at about 30° slope; Ellen, 1988.) Similar slope maxima for deep-seated failures are documented elsewhere (Brunori *et al*., 1996; Jennings and Siddle, 1998; Irigaray *et al*., 1999).

The variation of spatial frequency of landsliding with slope gradient, in one-degree increments, is systematic and nonlinear in the Oakland area. Frequency distributions for all but the smallest geologic units are near normal, as evident in Fig. 2 for the Orinda Formation (unit Tor). Spatial frequency of past landsliding

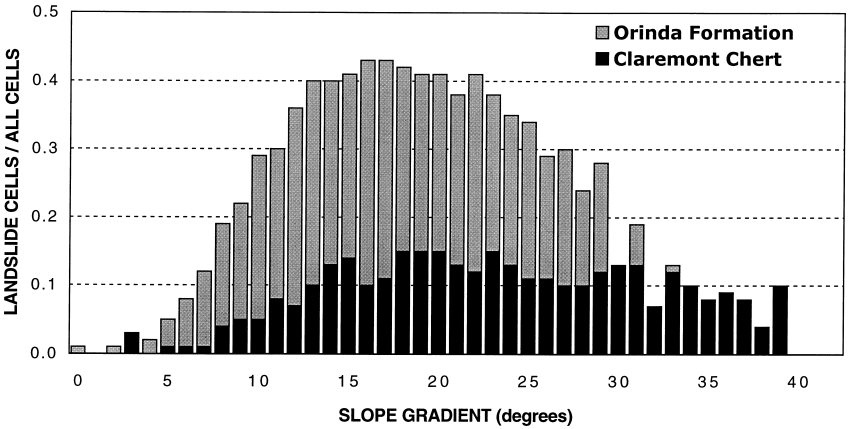


Fig. 2. Predisposition to landsliding can differ markedly by geology and slope gradient. Susceptibility, modeled as the number of 30-m grid cells on dormant landslide deposits divided by all cells, varies by 1° increments of slope in two of the 20 units in Table 1. The Claremont Chert (black, map unit Tcc) is much less susceptible than the Orinda Formation (gray, unit Tor). Mean spatial frequencies, respectively, are 0.11 and 0.28.

for unit Tor averages 28% (Table 1), but departs radically from the mean, rising from only 1% at zero slope to 43% at a slope of 16° and diminishing thereafter to <10% (Fig. 2). Collectively, the rising segments of all 120 such distributions include well over half the landslide cells in the study area, a correlation that supports some of the predictive capability claimed previously for slope gradient. The histogram for the 1192 post-1967 slides also has an overall bell-shape (Pike *et al.*, 2001). While frequencies of the steepest slopes in many units vary irregularly as the number of cells diminishes, these few aberrant values have little effect on later calculations. Distributions for the 32 units with <450 cells are more rectangular (Pike *et al.*, 2001) and resemble the histogram for steep slopes of the less susceptible (but overall steeper) Claremont Chert, unit Tcc in Fig. 2.

### *2. Between landslide deposits*

We calculated susceptibility both between and within landslide deposits in the Oakland area. Susceptibility *S* for grid cells not underlain by old slide masses (88% of the study area and 81% of its hilly terrain, Table 2) is estimated directly from the 120 distributions of spatial frequency by slope gradient. In the Orinda Formation, for example, where 29% of the 30-m cells sloping at 10° are located on old landslide deposits (Fig. 2), *all other* cells in unit Tor with a slope of 10° are assigned that same susceptibility *S*, of 0.29. In the less-susceptible Claremont Chert (unit Tcc), by contrast, only 5% of the cells in the 10° slope interval lie on mapped slide masses, whereupon an *S* of 0.05 is assigned to *all* remaining 10° cells in the Claremont. Values of *S*, determined slope interval-by-slope interval,

Table 2. Distribution of GIS grid cells and their susceptibility values $S_{ls}$ and $S$, by hillside or flatland sites and by location within or between old landslide deposits.

| Terrain and Geology | Number of 30-meter grid cells | | |
|---|---|---|---|
| | All cells | $S_{ls}$ - within slide deposits | $S$ - between slide deposits |
| Hillsides: the 100 bedrock units | 604,973 | 114,543 | 490,430 |
| Flatlands: the 20 surficial units | 364,030 | 1,817 | 362,213 |
| Entire study area: all 120 units | 969,003 | 116,360 | 852,643 |

are unique to each value of slope gradient in each of the 120 units. The resulting frequency distribution of susceptibility (not shown) for the 852,643 cells that lie between mapped landslide deposits is severely skewed, even in the log domain. Values range from $S$ = 0.00 for 300,000 cells in predominantly flat-lying Quaternary units to $S$ = 0.90 for 14 cells in unit Kfa, Alcatraz terrane (Table 1).

*3. Within landslide deposits*

Obtaining susceptibility $S_{ls}$, for the much smaller fraction of the area that is in landslide deposits (Table 2) is more complex. We first calculated raw susceptibility $S$ for the 116,360 cells within the deposits, by the same procedure as for cells between them. The highest $S$ on landslide masses is 1.00, for 70 cells (15 in unit Kfa) that occur in 21 different units. To estimate the higher susceptibilities that characterize dormant landslide deposits $S_{ls}$ we multiplied these 116,360 values of $S$ by a factor $a$, based on the relative frequency of recent failures in the region,

$$a = (\#hist_{ls}/A_{ls})/(\#hist_{nls}/A_{nls}) \quad (1)$$

where $\#hist_{ls}$ and $\#hist_{nls}$ are the numbers of recent failures within and outside old landslide deposits, respectively, and $A_{ls}$ and $A_{nls}$ are the areas (in number of cells) of old deposits and the terrain between them. This correction, (183/116,360)/(1009/852,643) or 1.33, indicates that recent landslides in the area are about 1/3 more likely to occur within old landslide deposits than between them. Lacking historic documentation of landsliding for each geologic unit, we applied the 1.33 multiplier to all 120 units. The highest value of $S_{ls}$ is 1.33, for the same 70 cells mentioned above. Because some $S_{ls}$ values exceed 1.00, all susceptibilities are expressed as decimals rather than percentages. Figure 3 combines values of $S$ and $S_{ls}$ to yield the frequency distribution of susceptibility for all 969,003 grid cells in the Oakland metropolitan area.

## EVALUATING THE MODEL

Landslide-susceptibility models are difficult to test; in actuality they can be "validated" only by the pattern of slopes that fail in subsequent storms and earthquakes. Two evaluations of our results for the Oakland area described in Pike *et al.* (2001) suggest that the model or a variant of it, with allowance for the effects of urbanization in Quaternary deposits, can estimate relative susceptibility, both within and outside the area in which the procedure was developed. Moreover, the modeled 33% higher incidence of recent failures within dormant slide deposits is of the magnitude noted previously for the area, about 55% to 70% in the more susceptible geologic units (Nilsen *et al.*, 1976, p. 19). Finally, Keefer *et al.* (1998, figure 4) found that 18 of the 20 largest landslides triggered in hills on the west side of San Francisco Bay by the 1989 Loma Prieta earthquake occurred within previous failures and occupied 55% of their area. Further development of the model is warranted. Distinguishing the inventoried landslides by triggering event (earthquake or precipitation) and type of movement, mapping a landslide's source area as well as its deposit (Wieczorek, 1984; Wilson *et al.*, 2002), and elaborating (if markedly complicating) the model by adding such variables as distance-to-nearest-road and terrain elevation, relief, aspect, and curvature from laser-generated DEMs are likely to strengthen the inferences.

## THE SUSCEPTIBILITY MAP

Pike *et al.* (2001) displayed the 969,003 values of susceptibility between ($S$) and within ($S_{ls}$) dormant landslide deposits in the test area as an eight-color map. In Fig. 1D the continuous range of values from 0.00 to 1.33 is shown in shades of gray for the same eight intervals, which widen with increasing susceptibility and decreasing number of cells. We chose the unequal intervals from inspection of the frequency distribution (Fig. 3) and test plots (not shown) to yield a balanced-appearing map that emphasizes the spatial variability of the index. We assigned no exact level of hazard to the eight intervals, but simply an increasing susceptibility from white (0.00) to black (≥0.55). Which intervals to label "safe" or "dangerous" is subjective and remains a matter of interpretation; no reliable calibration is available at this time. However, from field study that has long identified certain rocks in the Oakland area as susceptible (Nilsen *et al.*, 1976; Keefer and Johnson, 1983), $S$ and $S_{ls}$ values at least as low as 0.20 indicate areas of potential instability—depending on the strength and duration of triggering events. Dense clusters of values >0.30 are likely to indicate hazardous terrain.

The spatial patterns on this experimental map are not random. Figure 1 reveals slope instability controlled by geology and the resulting slope contrasts in the NW-SE-trending topography, particularly distribution of the steeper, higher ridges. Low susceptibilities of 0.05–0.20 predominate in the small sample shown in Fig. 1D, but values >0.30, which indicate high potential hazard and occupy 19% of metropolitan Oakland (30% of its hillside areas; Pike *et al.*, 2001), are conspicuous in steep terrain underlain by the Orinda Formation (Tor) in Fig.

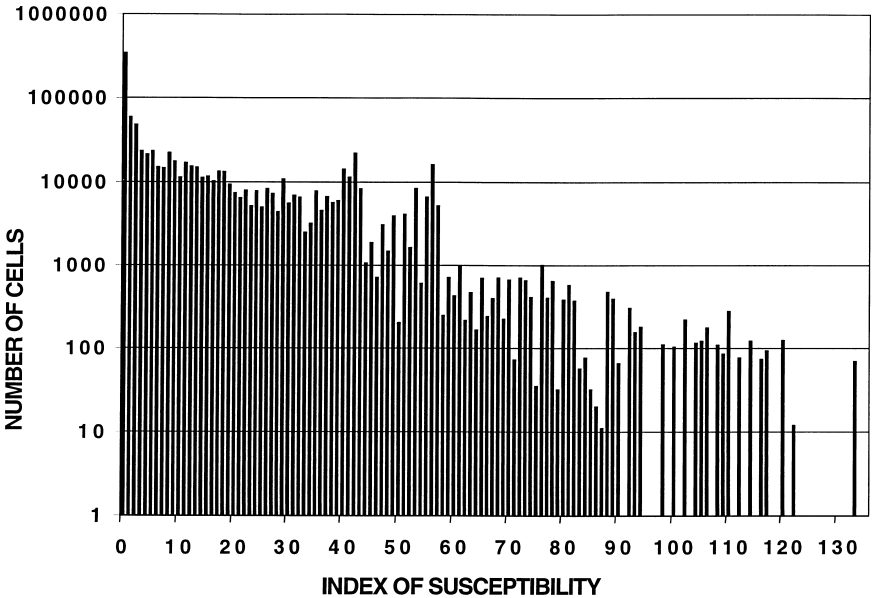


Fig. 3. Frequency distribution of susceptibility to large landslides for the 872 km$^2$ Oakland area, shown by log number of grid cells as a function of the modeled index number. This skewed histogram guided selection of the unequal intervals for mapping the susceptibility index (Fig. 1D).

1. Moreover, susceptibilities in the 0.10–0.29 range are common in Franciscan Complex mélange (KJfm) and other units (Table 1) that show evidence of failure (for more, see Pike *et al*., 2001). Most locations with the highest potential for hosting large landslides are steep and thinly settled, commonly in park land or tracts unlikely to be developed.

Areas of high susceptibility in Fig. 1D, while more likely to fail than locations with low values, also include local sites—scattered 30-m cells—that are not hazardous. More important for public safety, most low-susceptibility areas on the map are less prone to failure than areas of high value but are not without landslide hazard. Some of these locales slope steeply and are subject to debris flow (Ellen, 1988) and other types of failure—small landslides <60 m across, common in the area (Coe *et al*., 1999), were not included in the inventory on which Fig. 1D is based (Nilsen, 1975). Finally, landslide prediction remains something of an art, and the locus of much future landsliding cannot be identified with confidence. Slopes commonly fail from unanticipated blocking of surface drainage or other consequences of hillside development, as well as from random variation in the operation of landslide triggers and slope processes. Compiling Fig. 1D at a resolution coarser than 30 m might reflect some of these uncertainties.

## CONCLUSIONS

Various methods for mapping the landslide hazard have been proposed (Radbruch and Crowther, 1970; Brabb *et al*., 1972; Nilsen and Wright, 1979; Aniya, 1985; Dietrich *et al*., 1993; Brunori *et al*., 1996; Jennings and Siddle, 1998; Irigaray *et al*., 1999). All have advantages and disadvantages. Drawbacks to our regional approach for estimating susceptibility to landsliding include the need for accurate digital-map information on geology, terrain, and prior failure over a large area. We believe that these constraints, of input data rather than of the model, are outweighed by the method's conceptual advantages:

- the model can be computed quickly over a large area;
- extent of the area is limited only by that of the input data;
- areal coverage is 100%;
- Spatial resolution can be as fine as that of the DEM;
- both method and data are 100% quantitative;
- the susceptibility index is a continuous variable;
- the model yields a range of values within, as well as between, existing landslides;
- the model is more "transparent" than "black-box"; values of the index can be related directly to field observations; and
- the method is portable; it applies anywhere the necessary data are available (e.g., Pike and Sobieszczyk, 2002).

*Acknowledgements*—Prof. Michio Nogami and Nihon University generously supported R. J. Pike's attendance at the 5th ICG in Tokyo. Comments by USGS colleagues Jeff Coe and Ray Wilson and by Prof. Eiji Tokunaga improved earlier drafts of this chapter.

## REFERENCES

Aniya, M. (1985) Landslide-susceptibility mapping in the Amahata River basin, Japan: *Annals Assoc. American Geographers*, **75**, 102–114.

Brabb, E. E., Pampeyan, E. H. and Bonilla, M. G. (1972) Landslide susceptibility in San Mateo County, California: U.S. Geol. Survey Misc. Field Studies Map 360.

Brunori, F., Casagli, N., Fiaschi, S., Garzonio, C. A. and Moretti, S. (1996) Landslide hazard mapping in Tuscany, Italy—an example of automatic evaluation: In Slaymaker, O. (ed.), *Geomorphic Hazards*, pp. 56–67. Wiley, Chichester.

Coe, J. A., Godt, J. W., Brien, D. and Houdre, N. (1999) Map showing locations of damaging landslides in Alameda County, California, resulting from 1997–98 El Niño rainstorms: U.S. Geol. Survey, Misc. Field Studies Map 2325-B; http://pubs.usgs.gov/mf/1999/mf-2325-b/

Dietrich, W. E., Wilson, C. J., Montgomery, D. R. and McKean, J. (1993) Analysis of erosion thresholds, channel networks, and landscape morphology using a digital elevation model: *J. Geology*, **101**, 259–278; http://socrates.berkeley.edu/~geomorph/shalstab/

Ellen, S. D. (1988) Description and mechanics of soil slip/debris-flows in the storm: In Ellen, S. D. and Wieczorek, G. F. (eds.), *Landslides, Floods, and Marine Effects of the Storm of January 3–5, 1982, in the San Francisco Bay Region, California*: U.S. Geol. Survey Prof. Paper 1434, pp. 63–112.

Graham, S. E. and Pike, R. J. (1998) Slope maps of the San Francisco Bay region, California; a digital database: U.S. Geol. Survey Open-file Report 98-766, 17 pp.; http:wrgis.wr.usgs.gov/open-file/of98-766/index.html

Graymer, R. W. (2000) Geologic map of the Oakland Metropolitan Area, California: U.S. Geol. Survey, Misc. Field Studies Map 2342; http://geopubs.wr.usgs.gov/mapmf/mf2342/

Irigaray Fernández, C., Fernández del Castillo, T., El Hamdouni, R. and Chacón Montero, J. (1999) Verification of landslide susceptibility mapping—a case study: *Earth Surface Proc. and Landforms*, **24**, 537–544.

Jennings, P. J. and Siddle, H. J. (1998) Use of landslide inventory data to define the spatial location of landslide sites, South Wales, UK: In Maund, J. G. and Eddleston, M. (eds.), *Geohazards in Engineering Geology*, Eng. Geol. Spec. Publ. 15, Geological Society London, pp. 199–211.

Keefer, D. K. and Johnson, A. M. (1983) Earth flows-morphology, mobilization, and movement: U.S. Geol. Survey, Prof. Paper 1264, 56 pp.

Keefer, D. K., Griggs, G. B. and Harp, E. L. (1998) Large landslides near the San Andreas fault in the Summit Ridge area, Santa Cruz Mountains, California: In Keefer, D. K. (ed.), *The Loma Prieta, California, Earthquake of October 17, 1989—Landslides*: U.S. Geol. Survey, Prof. Paper 1551, C71–C128.

Lanyon, L. E. and Hall, G. F. (1983) Land-surface morphology 2, predicting potential landscape instability in eastern Ohio: *Soil Science*, **136**, 382–386.

Nilsen, T. H. (1973) Preliminary photointerpretation map of landslide and other surficial deposits of the Concord 15′ quadrangle and the Oakland West, Richmond, and part of the San Quentin 7.5′ quadrangles, Contra Costa and Alameda Counties, California: U.S. Geol. Survey Misc. Field Studies Map 493.

Nilsen, T. H. (1975) Preliminary photo-interpretation maps of landslide and other surficial deposits of 56 7.5-minute quadrangles, Alameda, Contra Costa, and Santa Clara Counties, California: U.S. Geol. Survey Open-File Report 75-277.

Nilsen, T. H. and Wright, R. H. (1979) Relative slope stability and land-use planning in the San Francisco Bay region, California: U.S. Geol. Survey Prof. Paper 944, 16–55.

Nilsen, T. H., Taylor, F. A. and Dean, R. M. (1976) Natural conditions that control landsliding in the San Francisco Bay region—an analysis based on data from the 1968–69 and 1972–73 rainy seasons: *U.S. Geol. Survey Bull.*, 1424, 35 pp.

Pike, R. J. and Sobieszczyk, S. (2002) A digital map of susceptibility to large landslides in Santa Clara County, California: *Eos Trans. American Geophys. Union*, **83**, 47 (Supplement), F557; http://www.agu.org/meetings/fm02/fm02-pdf/fm02_Hl2D.pdf

Pike, R. J., Graymer, R. W., Roberts, S., Kalman, N. B. and Sobieszczyk, S. (2001) Map and map database of susceptibility to slope failure by sliding and earthflow in the Oakland area, California: U.S. Geol. Survey, Misc. Field Studies Map 2385, 37 pp.; http://geopubs.wr.usgs.gov/map-mf/mf2385/

Pike, R. J., Howell, D. G. and Graymer, R. W. (2003) Landslides and cities—an unwanted partnership: In G. Heiken, R. Fakundiny and J. F. Sutter (eds.), *Earth Science in the City—A Reader*, American Geophys. Union Special Publication 56, pp. 187–254.

Radbruch, D. H. and Crowther, K. C. (1970) Map showing areas of relative amounts of landslides in California: U.S. Geol. Survey, Open-file Report OF 70-270, 36 pp.

Varnes, D. J. (1978) Slope movement and types and processes: In Schuster, R. L. and Krizek, R. J. (eds.), *Landslides—Analysis and Control, Special Report 176*, pp. 11–33. Transportation Research Board, National Academy of Sciences, Washington, D.C.

Wieczorek, G. F. (1984) Preparing a detailed landslide-inventory map for hazard evaluation and reduction: *Bull. Assoc. Eng. Geologists*, **21**, 337–342.

Wills, C. J. and McCrink, T. P. (2002) Comparing landslide inventories—the map depends on the method: *Environmental and Engineering Geoscience*, **8**, 279–295.

Wilson, R. I., Wiegers, M. O., McCrink, T. P., Haydon, W. D. and McMillan, J. R. (2002) Earthquake-induced landslide zones: In *Seismic hazard zone report for the Oakland East 7.5-minute quadrangle, Alameda County, California*, Seismic Hazard Zone Report 080, California Geological Survey, pp. 25–43 and Plate 2.1.